Leak-Tight Piezoelectric Microvalve for High-Pressure Gas Micropropulsion

Eui-Hyeok (EH) Yang, *Member, IEEE*, Choonsup Lee, Juergen Mueller, and Thomas George

***Abstract*—This paper describes the results of our development of a leak-tight piezoelectric microvalve, operating at extremely high upstream pressures for microspacecraft applications. The device is a normally closed microvalve assembled and fabricated primarily from micromachined silicon wafers. The microvalve consists of a custom-designed piezoelectric stack actuator bonded onto silicon valve components (such as the seat, boss, and tether) with the entire assembly contained within a stainless steel housing. The valve seat configurations include narrow-edge seating rings and tensile-stressed silicon tethers that enable the desired, normally closed, leak-tight operation. Leak testing of the microvalve was conducted using a helium leak detector and showed leak rates of 5×10^{-3} sccm at 800 psi (5.516 MPa). Dynamic microvalve operation (switching rates of up to 1 kHz) was successfully demonstrated for inlet pressures in the range of $0 \sim 1000$ psi. The measured static flow rate for the microvalve under an applied potential of 10 V was 52 sccm at an inlet pressure of 300 psi. The measured power consumption, in the fully open state, was 3 mW at an applied potential of 30 V. The measured dynamic power consumption was 180 mW for 100 Hz continuous operation at 100 psi. [1003]**

***Index Terms*—High pressure, micropropulsion, microvalve, piezoelectric.**

I. Introduction

CONSTELLATIONS of microspacecraft (each with 10 kg total mass) are being envisioned to study the magnetic fields or radiation belts surrounding the Earth [1]. Mission studies involving such spacecraft configurations are conducted by NASA under the Space Science Enterprise/Sun-Earth-Connection (SEC) Theme. By using large constellations of dozens, perhaps up to 100 spacecraft, tensor mapping of fields and particles over large regions of space will be possible. The Magnetic Constellation (Mag Con) mission, recently approved by NASA, seeks to map the Earth's magnetic field with 50–100 spacecraft, each equipped with its own magnetometer. Such large constellations of spacecraft are cost effective if individual, low mass spacecraft are used, to keep the total launch masses reasonable and, consequently, launch costs affordable. Thus, "Nanosat" architectures are being envisioned with total wet masses of about 10 kg per spacecraft. The Department of Defense (DoD) also has an interest in spacecraft constellations for Earth observation, ranging from 100-kg spacecraft in the TechSat 21 constellation to the "picosats," i.e., 1-kg total wet mass spacecraft being developed by the Defense Advanced Research Projects Agency (DARPA).

Manuscript received February 10, 2003; revised February 2004. This work was supported by a Contract from the National Aeronautics and Space Administration's Cross Enterprise Technology Development Program. Subject Editor F. K. Forster.

The authors are with the Jet Propulsion Laboratory, California Institute of Technology, Pasadena, CA 91109 USA (e-mail: Eui-Hyeok.Yang@jpl.nasa.gov).

Digital Object Identifier 10.1109/JMEMS.2004.835767

Table I classifies microspacecraft and distinguishes the various degrees of miniaturization and integration required [2].

Microspacecraft used in constellations will need propulsion either to maintain a formation or for attitude control, such as pointing an RF antenna to Earth for data transmission or aiming a camera for optical observations. Given the greatly reduced mass and size envelope of these spacecraft, significant reductions are needed in propulsion system size and mass over the current state-of-the-art. In addition, ultralow thrust and impulse bit capabilities will be needed for the lower mass spacecraft in order to achieve the necessary pointing accuracy. Table II lists the potential impulse bit requirements and required thrust levels for slewing ($180^\circ/\mathrm{min.}$) three generic cube-shaped spacecraft of 1-, 10-, and 20-kg mass, respectively, [1]. Also shown in the table are the various pointing (dead-band) requirements and time intervals between thruster firings. In general, longer times between thruster firings (so as to not disturb measurements, or to conserve propellant) necessitate lower rotation rates of the spacecraft as it drifts through the deadband, requiring therefore, that smaller impulse bits be imparted on the spacecraft. Thus, these impulse bits may range from the mNs-range for larger craft with relatively coarse attitude requirements, to the μNs-range and possibly even to the nNs-range for very tight pointing requirements and for very small spacecraft.

The discussion above presents the case for the development of very low impulse bit, micro-Newton thrust-level propulsion systems in order to meet the needs for pointing accuracy and attitude control for microspacecraft. Such micropropulsion systems will depend on precisely controlled, extremely low propellant flow from a pressurized propellant tank. A rapid-actuation, leak-tight microvalve capable of operating at high propellant pressures is therefore required for such micropropulsion systems (see microvalve requirements in Table III). Ideally, this valve will be tightly integrated into the propulsion system, making the overall thruster module compact and lightweight.

Significant efforts are needed for the development of high-pressure microvalves to meet the stringent micropropulsion requirements. Among other notable previous work described in the literature, the development of solenoid-actuated miniaturized valves has been reported [1]–[3]. Some of these valves meet most of the requirements for micropropulsion. However, these valves have relatively high power consumption, of the order of several Watts, during operation. Hand-in-hand with reductions in mass and size, microspacecraft systems are also anticipated to have severely limited power budgets. Therefore, low power consumption is an extremely desirable feature for microvalves that meet all of the other requirements for micropropulsion. Among the other previously reported microvalves, some have power consumption that is typically well within the

1057-7157/04$20.00 © 2004 IEEE

TABLE I
DEFINITION AND CLASSIFICATION OF MICROSPACECRAFT TYPES

Designation	S/C Mass (kg)	S/C Power (W)	S/C Dimension (m)	Comments
"Microspacecraft" (AF/European Definition)	10–100	10–100	0.3–2	Micropropulsion concepts beneficial due to weight/size savings.
"Class I Microspacecraft"	5–20	5–20	0.2–0.4	Use miniature "conventional" components. Conventional integration (e.g., feed lines) still possible, higher level of integration between components/subsystem desirable.
"Class II Microspacecraft"	1–5	1–5	0.1–0.2	Microfabricated components, high level of integration between components and subsystems required.
"Class III Microspacecraft" ("Nanosat")	< 1	< 1	< 0.1	All microfabricated. Very high level of integration between all subsystems and within subsystems required.

TABLE II
PROPULSION REQUIREMENTS FOR MICROSPACECRAFT

S/C Mass (kg)	S/C Typ. Dimension* (m)	Moment of Inertia (kg m^2)	Required Impulse Bit (Ns) 17 mrad (1°) 20 s	17 mrad (1°) 100 s	0.3 mrad (1 arcmin) 20 s	0.3 mrad (1 arcmin) 100 s	0.02 mrad (5 arcsec) 20 s	0.02 mrad (5 arcsec) 100 s	Minimum Thrust for Slew (mN)
1	0.1	0.017	1.4×10^{-4}	2.9×10^{-5}	2.5×10^{-6}	5.1×10^{-7}	1.7×10^{-7}	3.4×10^{-8}	0.06
10	0.3	0.150	4.3×10^{-4}	8.5×10^{-5}	7.5×10^{-6}	3.0×10^{-6}	1.0×10^{-6}	1.0×10^{-7}	1.75
20	0.4	0.533	1.1×10^{-3}	2.3×10^{-4}	2.0×10^{-5}	4.0×10^{-6}	1.3×10^{-6}	2.7×10^{-7}	4.65

* Assume cubical spacecraft shape

TABLE III
MICROVALVE REQUIREMENTS ARISING FROM NASA'S MINIATURE SPACECRAFT PROPULSION NEEDS, COMPARED WITH REPORTED PERFORMANCE TO DATE

Requirements	Target	Demonstrated
Leak rate	< 5×10^{-3} sccm/He	~ 5×10^{-3} sccm/He at 800 psi
Response time	< 10 ms	~30 µs
Inlet pressure	300~ 3000 psi	0~1000 psi
Power	< 1 W	~ 3 mW (static) at 30 V

low-power operation requirements. However, they do not meet either the requirements for the operating pressure range or for the ultralow leak rates needed for micropropulsion [4]–[14]. Recently, leak-tight microvalves operating at 10 atm (147 psi) have been reported [15]; however, even these operating pressures fall far short of the requirements. Thermally actuated microvalves usually have slow response times (> 100 ms to complete a cycle) [6]–[9], which is unacceptable for micropropulsion applications. Slower valve actuation time results in longer thruster on-times and consequently larger impulse bits. Thermally actuated valves also suffer the risk of random valve openings if ambient heating or cooling occurs, resulting in uncontrolled initiation of the actuation mechanism. Most microvalves reported previously have shown poor valve seating at high pressures, resulting in severe leakage problems and inadequate pressure handling capability. In this paper, we describe the design, fabrication, and characterization results for a low-power, leak-tight, piezoelectric microvalve, operating under extremely high inlet pressures for micropropulsion applications.

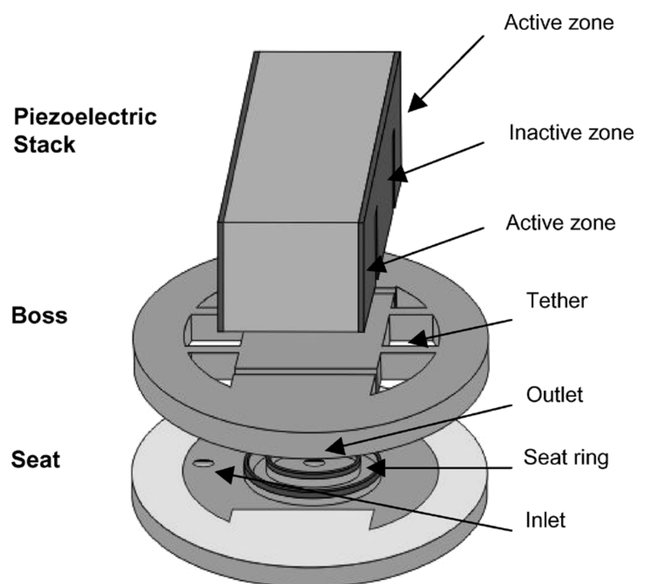

Fig. 1. Conceptual schematic of the JPL piezoelectric microvalve.

TABLE IV
SPECIFICATIONS FOR THE CUSTOM-DESIGNED PIEZOELECTRIC STACK ACTUATOR

Properties	Specifications
Piezoelectric material	Soft doped PZT – S2
Dimension – Cross section	8.4 mm x 5 mm (ceramic)
Dimension – Height	6 mm
Special dimensional features	Two slots 0.3-mm wide and 5.5-mm deep, separating the inactive center zone from the two active zones.
Maximum voltage	+60 V
Maximum displacement	-1 µm @ -10 V and 5 µm @ 60 V
Blocking force	1000 N
Capacitance	1700 nF
Curie temperature	235°C
Maximum operating temp.	125°C

II. MICROVALVE DESIGN

The core components of a piezoelectric microvalve described in this paper are a seat plate, a boss plate, and an actuator as shown in Fig. 1. The microvalve components avoid the use of fragile membranes in order to allow high-pressure operation. Major elements of the microvalve design include the custom designed piezoelectric stack actuator and the seating configuration consisting of narrow seat rings.

Table IV contains detailed specifications of the piezoelectric stack actuator (vendor: Noliac A/S, Denmark) with dimensional parameters. The stack actuator exhibits a very high block-force ($\sim$ 1 kN), and thus is capable of generating a valve-opening pressure far greater than the seating pressure made up of the combined inlet gas pressure and the initial seating pressure arising from the tensile-stressed silicon tether suspension. The custom-designed stack of piezoelectric actuators consists of peripheral active zones and an inactive central zone. The active zones are mechanically separated (by deep U-grooves) from the central, inactive zone. These zones are bonded to corresponding peripheral and central areas of the boss plate. Application of a voltage ($\sim$ 60 V) to the piezoelectric stack causes the active zones to vertically expand by 5 μm, lifting the boss center plate (bonded to the inactive zone), away from the seat plate.This actuation creates a channel between the two seating surfaces, permitting the passage of fluids as shown in Fig. 2. Since the piezoelectric actuator is essentially a stacked capacitor, it consumes extremely low power when it is not moving, thus allowing a near zero-power, open or closed operation for the microvalve.

A concentric series of narrow rings on the seat plate (10 rings total) is designed to provide the redundancy necessary to maintain a leak-tight operation in the event of damage to individual seating rings. The narrow rings (1.5 μm wide and 10 μm deep) simulate a "knife-edge" seal by reducing the contact area, thereby increasing the seating pressure and consequently reducing internal leaks. The center portion of the boss plate has a 2-μm-thick silicon dioxide layer functioning as a hard seat coating material. The boss plate is bonded to the seat plate via metal-to-metal compression along the periphery. The thickness of the silicon dioxide coating on the boss plate varies, being slightly thicker (2 μm) in the center than at the periphery. This oxide thickness difference results in the generation of tensile stress in the silicon tether suspension. The tensile stressed silicon tether suspension of the boss plate provides an initial valve-seating pressure as shown in Fig. 3. The estimated maximum tensile-stresses in the tethers, obtained from an ANSYS simulation, are approximately 80 MPa and 16 MPa during the on-state and the off-state, respectively. These are far lower than the fracture stress of silicon ($\sim$ 7 GPa), thus enabling reliable long-term on-off actuation. Estimated seating pressure from the tethers on the seating rings is approximately 88 kPa for the normally closed operation.

The dominant seating pressure is, in fact, applied by the piezoelectric actuator during the as-closed-state of the microvalve. This seating pressure is achieved using the following fabrication and assembly procedure: A voltage of 10 V is applied initially to the piezoelectric stack actuator during bonding onto the boss plate. Once bonded, this assembly procedure insures that the boss plate is pressed onto the seat plate by the inactive zone (attached to the boss center plate) of the piezoelectric stack prior to the microvalve operation. Our estimate of this initial valve-closing pressure is approximately 954 MPa and far exceeds the other sources, described above, for the seating pressure.

III. FABRICATION OF THE MICROVALVE

The silicon components of the microvalve are fabricated primarily by deep trench etching (reactive ion etching), deposition, and patterning processes. The fabrication process sequence for the silicon components is described in Fig. 4.

All silicon wafers (300 μm thick) for the valve seat and boss plates are thermally oxidized (0.5 μm). The seating rings are first lithographically defined on the valve seat wafer [Fig. 4(a)]. The silicon dioxide layer is selectively removed in 10:1 buffered oxide etchant (BOE) for 10 min. The wafer is then etched using deep reactive ion etcher (DRIE), in order to generate 10 μm deep seating ring structures [Fig. 4(b)]. Next, the seat wafer is metallized with Cr/Pt/Au (0.03 μm/ 0.06 μm/ 0.25 μm) and patterned to define the bonding surfaces [Fig. 4(c)]. The seat wafer is then subsequently etched from the backside using DRIE, to open up vias for the inlet and outlet ports [Fig. 4(d)].

A 2-μm-thick silicon dioxide is grown by plasma enhanced chemical vapor deposition (PECVD) and patterned on the boss wafer. The oxide layer is etched in BOE (10:1) for 40 min. The bonding metals (Cr/Pt/Au) are deposited subsequently and patterned on the periphery of the boss plate [Fig. 4(e)]. The boss wafer is then patterned to define the boss (or valve flap and tethers), which is released in a final DRIE process [Fig. 4(f)].

The boss and seat wafers are bonded to create a sealed, yet movable structure [Fig. 4(g)]. An Electronic Visions aligner and thermocompression bonder are used to align and bond the two wafers. The bonder chamber is pumped down to 1×10^{-5} torr prior to the bonding operation. A piston pressure of 1 MPa is applied at 380 °C in the vacuum chamber to provide the necessary thermocompression bonding force. Then, the piezoelectric stack actuator is carefully aligned (using a specially designed

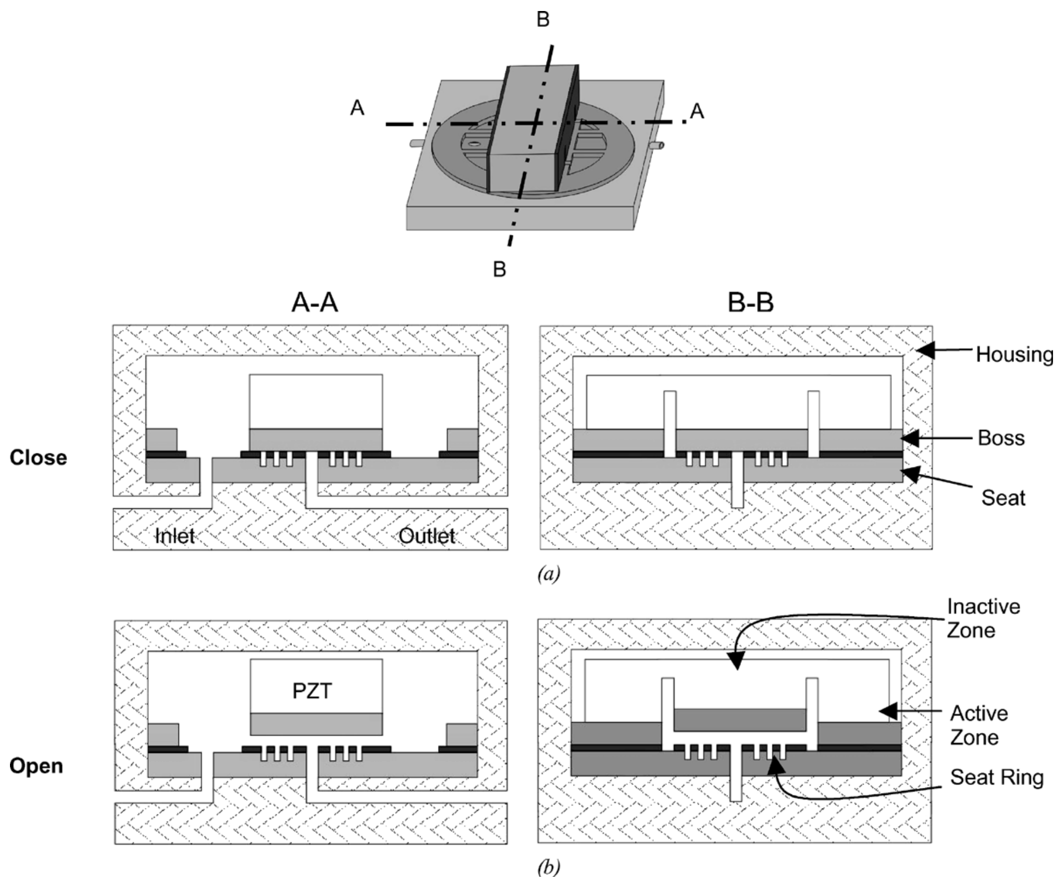

Fig. 2. Operating principle of the normally closed, leak-tight, high-pressure, piezoelectric microvalve. Applying a voltage ($\sim$ 60 V) to the piezoelectric stack makes the active zones dilate by 5 μm, lifting the center boss plate (bonded to the inactive zone of the stack) away from the seat plate.Thus, a channel is created between the two plate surfaces, allowing for the passage of fluids. (a) Microvalve closed (cross section A-A). (b) Microvalve opened (cross section B-B).

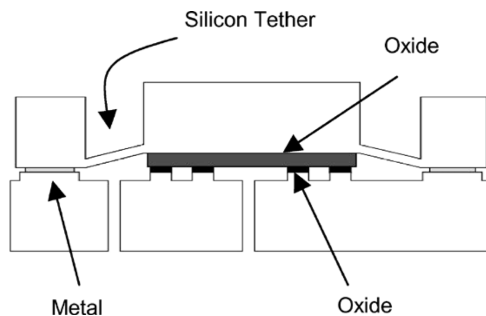

Fig. 3. Cross-sectional microvalve configuration, showing the suspension of the boss plate by tensile stressed silicon tethers over the extended valve seat.

jig) and bonded onto the center top of the boss plate using an epoxy (Hysol E/A 9394, cured at room temperature). Finally, the microfabricated valve components are bonded to stainless steel fixtures, which are then hermetically sealed using the same epoxy.

Fig. 5 contains scanning electron micrographs (SEM) of the silicon components of a microvalve. Fig. 6 is a photograph of the fully packaged microvalve.

IV. Characterization and Discussion

A. Test Setup

The fully assembled microvalves were tested under inlet pressures of up to 1000 psi. Testing of the microvalve at higher pressures was not possible because 1000 psi is the safety limit of our current test setup. Fig. 7 shows a schematic of the high-pressure valve test bench. A helium (He) gas based test apparatus was used for the leak and flow testing of the microvalves.

B. Leak and Flow Characteristics

We have fabricated and assembled 3 microvalves. They all showed similar and good performance when we tested for leaks at inlet pressures in the range of 300–600 psi (in 100 psi increments). However, given our constraints in time and budget, it was possible to thoroughly test only one of these valves. We expended considerable effort in developing a protocol to test the valve for inlet pressures in the range from 0–1000 psi, in 20 psi increments up to 150 psi, and thereafter in 100 psi increments up to 1000 psi.

Leak testing of a microvalve using a helium leak detector showed an extremely low leak rate of 5×10^{-3} sccm at an inlet pressure of 800 psi. Fig. 8 shows the leak rates of the microvalve for various inlet pressures. The high seating pressure generated by the piezoelectric stack actuator is responsible for the extremely low leak rates. Fig. 9 contains the static forward flow rates for an actuated microvalve for various actuation voltages and inlet pressures. Measured flow rates, at an actuation voltage of 10 V, are approximately 52 sccm at an inlet pressure of 300 psi. Fig. 10 shows the flow rates for a microvalve actuated in a pulsed mode. In Fig. 9, for an inlet pressure of 100 psi and

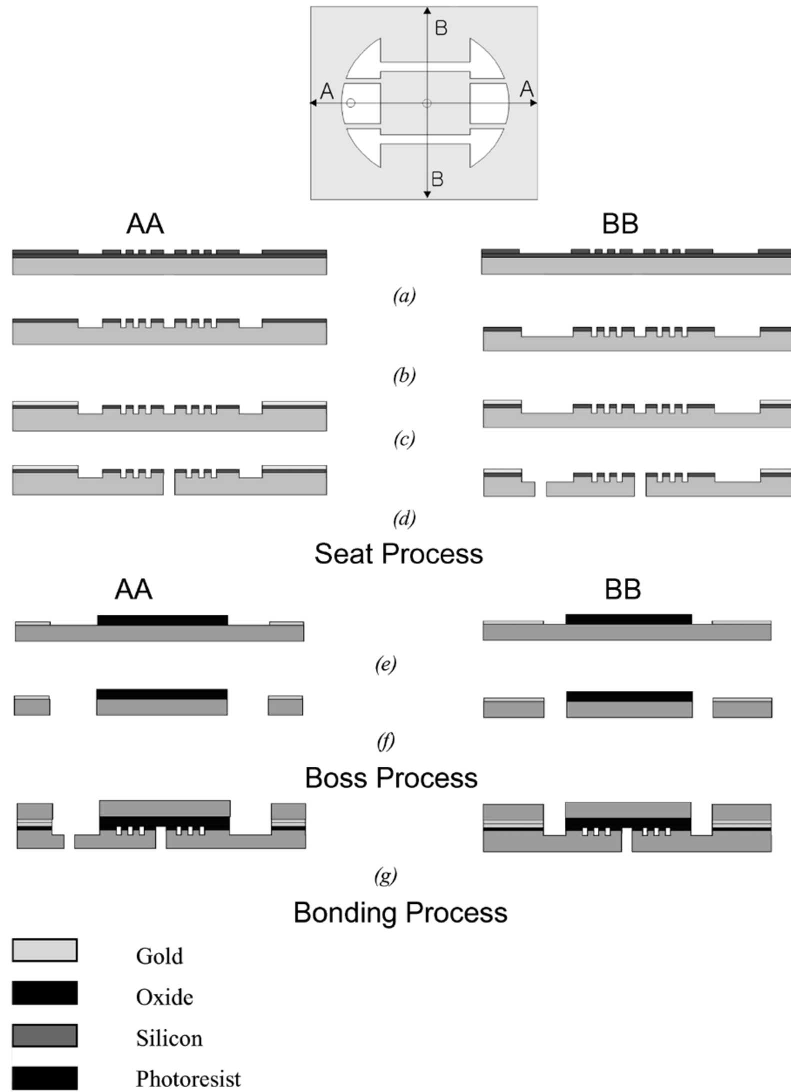

Fig. 4. Fabrication sequence. (a) The seating rings are lithographically defined on the valve seat wafer. (b) After the removal of oxide, the 10-$\mu\mathrm{m}$ deep valve seat ring structures are fabricated by DRIE. (c) The wafer is metallized and patterned to define the bonding surfaces. (d) The seat wafer is etched from the backside using DRIE in order to open up vias for the inlet and outlet ports. (e) A silicon dioxide layer is deposited and patterned on the boss wafer. The bonding metals are deposited and patterned on the periphery of the boss plate. (f) The boss (or valve flap and tethers) wafer is then patterned to define the boss, which is released in a final DRIE process. (g) The boss and seat wafers are bonded.

an applied dc actuation voltage of 10 V, the measured flow rate is approximately 20 sccm. In a 10-Hz pulsed operation mode as shown in Fig. 10, however, the flow rate was measured to be approximately 7.7 sccm for a 90% duty cycle. Measurements made at constant duty cycle and constant inlet pressure show that the flow rate drops significantly with higher frequency operation. Thus, these measurements demonstrate that on average, the valve opening, and hence the flow rate, is reduced for cyclic 10-V operations as compared to the static actuation case.

Fig. 11 contains the flow rates obtained for valve operating frequencies from 10 Hz to 10 kHz using a sinusoidal actuation voltage with an amplitude of 10 V. In general, for a given inlet pressure, the flow rate decreases with higher operating frequency as discussed earlier. However, for an inlet pressure of 100 psi, an anomalous increase is first observed in the flow rate with increasing operating frequency, reaching a maximum value at approximately 300 Hz. Such anomalous trends have been observed previously in pulsating flows within ducts with immovable walls [16]. In our case, the movement of the boss plate could cause the instantaneous volume of the flow passage to vary with time, resulting in flow characteristics similar to a condition known as squeeze flow [17]. Detailed modeling of the dynamic operation using computational fluid dynamics (CFD) analysis would be necessary to completely understand this phenomenon; however, this is beyond the scope of the current work.

C. Cyclic Performance Evaluation

After the series of flow tests described above, a cycling test was performed for 10^5 cycles using the same microvalve. The microvalve was connected to a Helium gas tank regulated at 100 psi, and was actuated with an applied 1 Hz, 10 V square wave. After 10^5 cycles operation, the leak rates were measured again. No significant degradation was observed in the leak rate in the as-closed state.

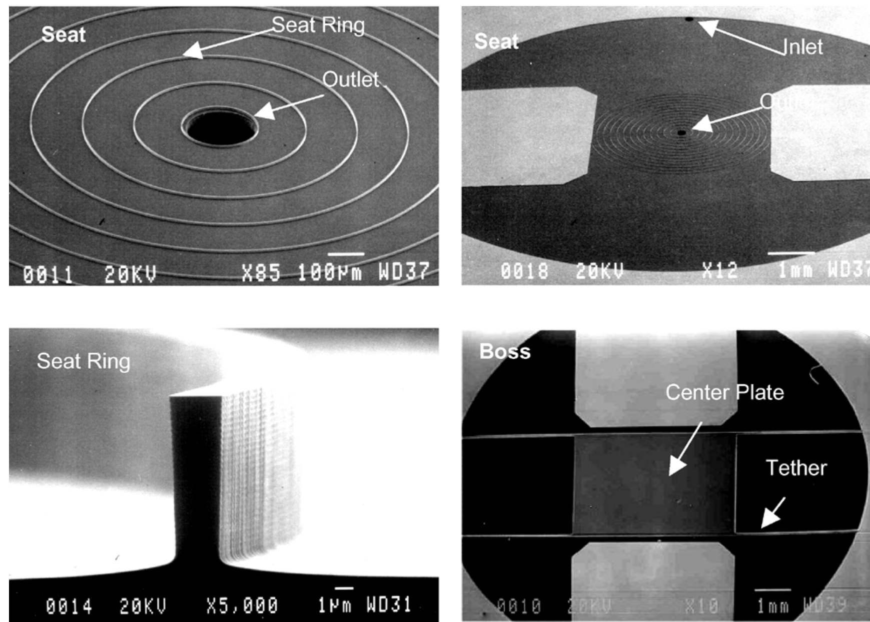

Fig. 5. Scanning electron micrographs of the seat plate and the boss plate. The top surfaces of the seat rings are covered with a 0.5-μm-thick thermal oxide.

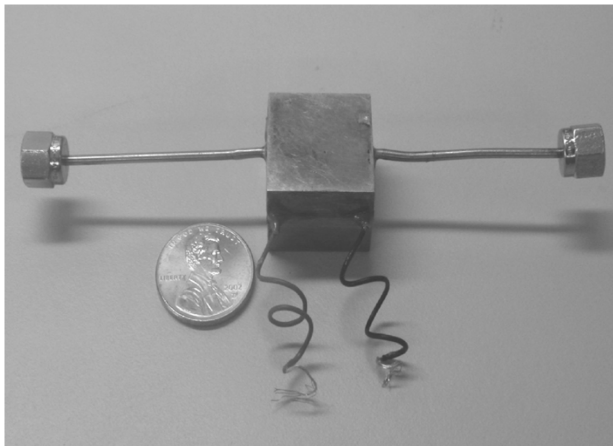

Fig. 6. Packaged high-pressure piezoelectric microvalve.

Inspection by SEM after these tests was not done, since degradation in performance was not observed.We were unable to determine the cause by the appearance of the seat ring area, when we examined the region for another microvalve that exhibited a higher leak rate during the development of the cycling test protocol.

A series of tests (using a calibrated Met One A2408 particle counter) was conducted to determine the particle size range, flowing from the Helium gas tank. The measured average particle size and count are listed in Table V. It appears that the particles in the He gas tank used for the testing are smaller than 1 μm in size. The successful cyclic operation and leak-tight performance of the microvalves clearly demonstrate that the devices can perform reliably in the presence of small ($< 1\ \mu$m) particulates within the gaseous effluents. In the case of flows containing larger particles, appropriate levels of prefiltering may be necessary in order to ensure reliable operation of the microvalves.

D. Seating Pressure

Proper control of seating pressures is critical in order to reduce the leak rates from microvalves. For conventional, soft seat valves, a seating pressure of ~ 100 kPa is sufficient for high-pressure applications. For hard seat applications however, seating pressures in excess of 100 MPa are desirable [2]. In the present case, by actuating the piezoelectric stack during bonding, we were able to generate an initial valve-seating pressure of approximately 954 MPa. The seating pressure is produced in the following way: A 10-V potential is applied to the piezoelectric actuator stack during bonding with the silicon valve components. The purpose of this initial bias is that the piezoelectric actuator applies the maximum valve seating force estimated at 200 N (from the vendor specifications) when the bias is removed. This initial seating force therefore corresponds to approximately 954 MPa seating pressure on the valve seat. This seating pressure is far greater than previously reported seating pressures for hard seat valves, thereby ensuring a leak-tight, normally closed state under high inlet pressures.

E. Power Consumption

Piezoelectric valves offer significant advantages over solenoid-actuated valves for proportional flow control. In general, solenoid valves require operation in a pulse width modulation mode in order to provide the necessary proportional flow control. Piezoelectric microvalves, on the other hand, do not require pulse width modulation because the actuation is directly proportional to the applied voltage. Since the power consumption of a static piezoelectric actuator is negligible, nearly zero-power microvalve operation is possible during the firing of microthrusters. The measured static (dc) power consumption

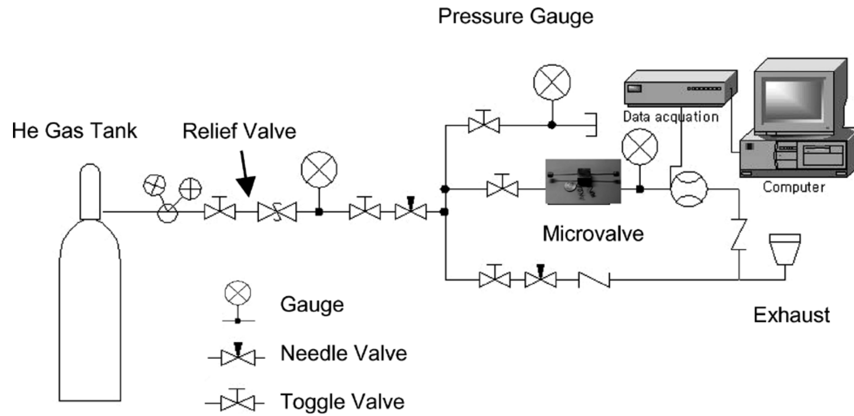

Fig. 7. Schematic diagram of high-pressure flow test bench for microvalve characterization.

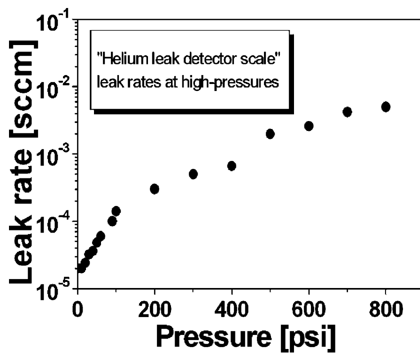

Fig. 8. Measured internal leak rate for a normally closed (nonactuated) microvalve is approximately 5×10^{-3} sccm at an inlet pressure of 800 psi.

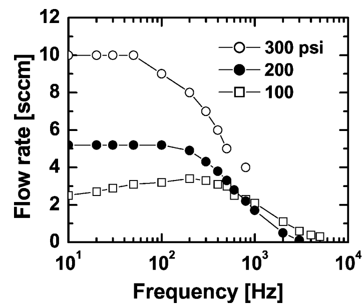

Fig. 11. Measured flow rates for a microvalve operating over a wide frequency range, demonstrating that fast ($\sim$ 30 μs) valve operation is indeed possible. (Actuation using a 10-V amplitude sine wave).

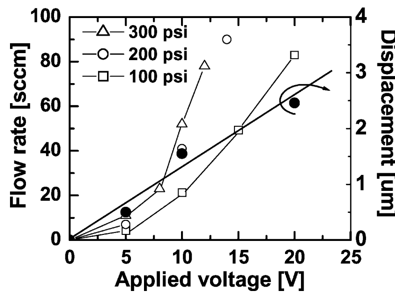

Fig. 9. Measured flow rates for an actuated microvalve. Piezoelectric actuation has been successfully demonstrated for inlet pressures in the range of $0 \sim 1000$ psi. Flow rates at inlet pressures above 300 psi are above the measurement range of the flow meter used in the tests.

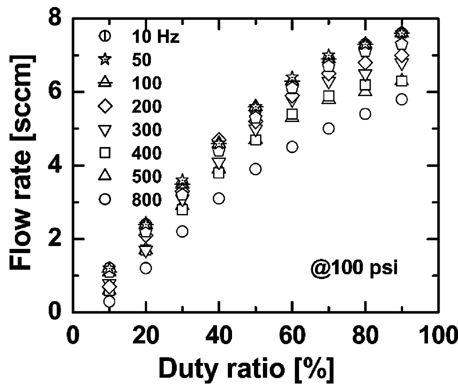

Fig. 10. Measured flow rates for a microvalve actuated in a pulsed mode at 100 psi. (A 10 V square wave actuation pulse was applied).

TABLE V
MEASURED PARTICLE COUNT IN THE HELIUM TANK USED FOR MICROVALVE FLOW CHARACTERIZATION. THE TEST RESULTS SHOW THAT THE MOST PARTICLES IN THE HELIUM GAS TANK ARE SMALLER THAN 1 μm. APPROPRIATE PRE-FILTRATION MAY BE REQUIRED FOR RELIABLE MICROVALVE OPERATION WHEN USING EFFLUENTS CONTAINING LARGER PARTICULATES

Particle Size Range and Number of Particles per 0.99 CFM		
Size (μm)	Cumulative	Differential
0.3	153.7	138.9
0.5	14.9	11.7
1.0	3.2	2.9
3.0	0.3	0.1
5.0	0.2	0.1
>10.0	0.1	0.1

CFM: Cubic Feet per Minutes.

Differential: number of particles in the particular range

Cumulative: differential + all the smaller particles added.

required to keep the microvalve fully open is about 3 mW at 30 V. This static power consumption is primarily due to leakage currents in the piezoelectric stack. The dynamic (ac) power consumption of the piezoelectric microvalve, resulting from dissipation during charging and discharging the stacked capacitor, is approximately 180 mW at 100 Hz.

V. Conclusion

A leak-tight, high-pressure piezoelectric microvalve technology has been demonstrated for low impulse-bit micropropulsion applications. Thus, these microvalves will enable low impulse-bit thruster modules for use in very small spacecraft as well as for providing precise attitude control functions for larger spacecraft. The promising results from the microvalve characterization described in this paper provide the assurance that it is indeed possible to meet the demanding requirements of NASA's next-generation microspacecraft architectures. The microvalve incorporates a custom-designed piezoelectric stack actuator to provide the actuation forces necessary for high-pressure operation. A hard seating configuration using a series of narrow concentric seating rings contributes to the enhanced leak-tight microvalve operation. Extremely low leak rates of 5×10^{-3} sccm were demonstrated for an inlet pressure of 800 psi. Reliable and reproducible microvalve operation has been demonstrated. The availability of such microvalves is expected to "open several doors" among microfluidics applications. The microvalve technology demonstrated here is amenable to integration with fluidic devices and with other MEMS components.

Acknowledgment

The authors thank L. Wild and D. Bame at the Jet Propulsion Laboratory for their support during the assembly and flow tests. The authors also thank Prof. J. M. Khodadadi of Auburn University for his valuable technical comments on dynamic flow behavior.

References

[1] J. Mueller, C. Marrese, J. Ziemer, A. Green, E. H. Yang, M. Mojarradi, T. Johnson, V. White, D. Bame, R. Wirz, M. Tajmar, V. Hruby, M. Gamero-Castaño, J. Schein, and R. Reinicke, "JPL micro-thrust propulsion activities," in *Nanotech 2002*, Houston, TX, Sept. 9–12, 2002, AIAA Paper 2002-5714.

[2] J. Mueller, "A review and applicability assessment of MEMS-based microvalve technologies for microspacecraft propulsion," in *Micropropulsion for Small Spacecraft*, M. Micci and A. Ketsdever, Eds. Reston, VA: AIAA, 2000, vol. 187, Progress in Astronautics and Aeronautics, ch. 19.

[3] ——, "Thruster options for microspacecraft: A review and evaluation of existing hardware and emerging technologies," in *Micropropulsion for Small Spacecraft*, M Micci and A Ketsdever, Eds. Reston, VA: AIAA, 2000, vol. 187, Progress in Astronautics and Aeronautics, ch. 3.

[4] K. Yanagisaa, H. Kuwano, and A. Tago, "Electromagnetically driven microvalve," *Microsyst. Technol.*, vol. 2, no. 1, pp. 22–25, 1995.

[5] P. Dubois, B. Guldimann, M.-A. Gretillat, and N. F. de Rooij, "Electrostatically actuated gas microvalve based on a Ta-Si-N membrane," in *Proc. 14th IEEE MEMS 2001 Tech. Dig.*, 2001, pp. 535–538.

[6] S. Messner, M. Muller, V. Burger, J. Schaible, H. Sandmaier, and R. Zengerle, "A normally-closed, bimetallically actuated 3-way microvalve for pneumatic applications," in *Proc. 11th IEEE MEMS 1998 Tech. Dig.*, Heidelberg, Germany, 1998, pp. 40–44.

[7] K. D. Ksrobanek, M. Kohl, and S. Miyazaki, "Stress-Optimized shape memory microvalves," in *Proc. 10th IEEE MEMS 1997 Tech. Dig.*, 1997, pp. 256–261.

[8] P. W. Barth, "Silicon microvalves for gas flow control," in *Transducers '95*, Stockholm, Sweden, 1995, pp. 276–279.

[9] M. J. Zdeblick, R. Anderson, J. Jankowski, B. Kline-Schoder, L. Christel, R. Miles, and W. Weber, "Thermopneumatically actuated microvalves and integrated electro-fluidic circuits," in *IEEE Solid-State Sensor and Actuator Workshop 1994 Tech. Dig.*, Hilton Head Island, SC, 1994, pp. 251–255.

[10] D. Johnson, "Valves for instrumentation and propulsion systems in microspacecraft," in *Proc. 9th Adv. Space Propulsion Workshop*, Pasadena, JPL D-15 671.

[11] M. A. Huff, J. Gilbert, and M. A. Schmidt, "Flow characteristics of a pressure-balanced microvalve," in *Transducers' 93*, Yokohama, Japan, 1993, pp. 98–101.

[12] D. Bosch, B. Heimhofer, G. Muck, H. Seidel, U. Thumser, and W. Welser, "A silicon microvalve with combined electromagnetic/electrostatic actuation," *Sens. Actuators*, vol. 37–38, pp. 684–692, 1993.

[13] M. Shikida, K. Sato, S. Tanaka, Y. Kawamura, and Y. Fujisaki, "Electrostatically-actuated gas valve with large conductance," in *Transducers' 93*, Yokohama, Japan, 1993, pp. 94–97.

[14] M. Esahi, S. Shoji, and A. Nakano, "Normally-closed microvalve and micropump fabricated on a silicon wafer," *Sens. Actuators*, vol. 20, pp. 163–169, 1989.

[15] X. Yang, A. Holke, and M. A. Schmidt, "An electrostatic, on/off MEMS valve for gas fuel delivery of a microengine," in *Solid-State Sensor and Actuator Workshop*, Hilton Head Island, SC, June 2–6, 2002, pp. 19–22.

[16] J. M. Khodadadi, "Oscillatory fluid flow through a porous medium channel bounded by two impermeable parallel plates," *J. Fluids Eng.*, vol. 113, pp. 509–511, 1991.

[17] F. M. White, *Viscous Fluid Flow*, 2nd ed. New York: McGraw-Hill, 1991.

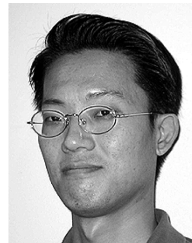

Eui-Hyeok (EH) Yang (M'03) received the B.S., M.S., and Ph.D. degrees from the Department of Control and Instrumentation Engineering, Ajou University, Korea, in 1990, 1992, and 1996, respectively.

He joined the Fujita MEMS Research Group, Institute of Industrial Science, University of Tokyo, Japan, as a Visiting Postdoctoral Researcher in 1999. He received a research fellowship from the Japan Society for the Promotion of Science from 1996 to 1998. Since 1999, he has been with the Jet Propulsion Laboratory (JPL), Pasadena, CA, where he initiated the development of MEMS adaptive optical devices. He has recently been granted several competitive proposals. He is a technical monitor for a NASA SBIR project for the development of actuators for optical mirror devices. He has participated in development of several electrostatic, thermopneumatic, piezoelectric, and shape memory alloy devices for microfluidics systems, inertial microsensors, and optical MEMS devices. He is currently a Senior Member of the Engineering Staff at NASA's JPL, and the task manager for several MEMS technology development projects. He has extensive experience in MEMS actuator, deformable mirror, and optical membrane fabrication. He is leading the development of MEMS-based deformable mirrors and actuators for future large aperture telescopes. He is also leading the development of MEMS-based piezoelectric valves for future microspacecraft applications. He participated in the technical evaluation of MEMS mirror array technologies being developed for the Multi Object Spectrometer (MOS) project for the James Webb Space Telescope (JWST). He has successfully developed a membrane-transfer technology for large-area deformable mirrors that is being targeted for ultralarge space telescopes. His current research focuses on microactuators, fluidic microsystems, and adaptive optics for space applications.

Dr. Yang is a member of the Technical Program Committee for the IEEE Sensor Conference and the SPIE Micromachining and Microfabrication Conference. He is a recipient of the Lew Allen Award for Excellence at JPL.

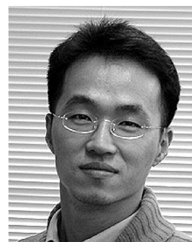

Choonsup Lee received the B.S. degree in electrical engineering from the Kyoungpook National University in 1996. He received the M.S. and Ph.D. degrees in electrical engineering from the Korea Advanced Institute and Science and Technology (KAIST) in1998 and 2002, respectively. He also

He is a California Institute of Technology Postdoctoral Scholar with the Jet Propulsion Laboratory (JPL), Pasadena. He joined the MEMS Technology Group at JPL in 2002. He has extensive experience in the design and characterization of microsensors and microactuators such as thermal inkjet printhead, force-balanced tunneling microaccelerometer, infrared detector, silicon microlens, MEMS-based band-pass filter, microvalve, nanochannel, lateral field emission device, and other MEMS/NEMS devices. Currently, he is working on microfluidic/nanofluidic devices and nanowire-based sensors. He has published 10 international journal papers and 11 refereed conference publications.

Juergen Mueller, photograph and biography not available at the time of publication.

Thomas George received the B.Tech. degree from the Indian Institute of Technology, Madras, and the M.S. and Ph.D. degrees in materials science from the University of California, Berkeley.

He is the Supervisor of the MEMS Technology Group at NASA's Jet Propulsion Laboratory, Pasadena, CA. He has established and manages a multidisciplinary group consisting of 22 researchers working on the development of diverse MEMS/NEMS technologies for NASA applications. The group pursues end-to-end development from concepts to implementation in space missions. R&D efforts are directed toward effectively exploiting new phenomena at micro- and nanoscales in order to create novel sensors and actuators. The MEMS technologies being developed by the group include microgyroscopes, micropropulsion devices, microvalves, microinstruments, Bio-MEMS, and NEMS resonators. Currently, he serves as the Chair of the MEMS Review Board (MRB) for the James Webb Space Telescope project. The review board includes MEMS experts from Sandia National Laboratories and the University of Maine, as well as astronomers and system developers. The MRB, under his leadership, was responsible for downselecting the Micro-Shutter Array concept being developed by NASA's Goddard Space Flight Center from among three possible MEMS array options for the Near Infrared Multi-Object Spectrometer (NIR-MOS). The MRB's current role is to review the progress being made on the Micro-Shutter Array project. He cofounded the Canada-Europe-US-Japan (CANEUS) organization to promote the rapid and cost-effective transition of Micro-Nano Technologies (MNT) for Aerospace applications. He holds five U.S. patents and has coauthored more than 90 publications.

Dr. George has participated as Principal Investigator/Co-Investigator on numerous R&D proposals and has put together multiinstitution, multidisciplinary teams in response to proposal opportunities with various governmental agencies and commercial sponsors. He led the the joint development by JPL and the Aerospace Corporation of a MEMS-based PICOSAT satellite for a DARPA/AFRL sponsor. The PICOSAT was developed as a low-cost, rapid, space-testing platform for testing a wide range of MEMS technologies and mission architectures. He coorganized the CANEUS 2002 and is in the process of organizing the CANEUS-2004 conference aimed at brining together international, complementary core-competencies from institutions across the participating, member countries for rapid prototype development of MNT-based systems and subsystems.